

Technical note

Semi-automatic design concept of 3D-printed individualized template for interstitial brachytherapy of vaginal tumors

Shuhei Sekii^{a,b,c,*}, Kento Morita^d, Ryuichi Yada^e, Kayoko Tsujino^b^a Department of Radiation Oncology, Kita-Harima Medical Center, Hyogo, Japan^b Department of Radiation Oncology, Hyogo Cancer Center, Hyogo, Japan^c Department of Radiation Oncology, Osaka Police Hospital, Osaka, Japan^d Department of Information Engineering, Graduate School of Engineering, Mie University, Mie, Japan^e Department of Regional Medical Management Studies, Hamamatsu University School of Medicine, Shizuoka, Japan

ARTICLE INFO

Keywords:

Additive manufacturing
3D printing
Radiation oncology
Gynecology
Brachytherapy
Cervical cancer
Endometrial cancer
Vaginal cancer

ABSTRACT

We aimed to introduce a novel semi-automatic design approach for fabricating individualized, three-dimensional printed template dedicated to interstitial brachytherapy in vaginal tumor treatment. The central component of this concept involved the development of a cylindrical template with strategically placed tunnels to optimize applicator placement. These tunnels originated from the template's base, meticulously designed to prevent any potential overlap or interference. For precise tumor localization, we employed a method wherein the tumor's mask image was projected onto a spherical surface. Subsequently, we employed the k-means algorithm to segment the terminal points, with each cluster's center serving as the terminal point. To ensure the optimal starting point for the tunnels, we utilized the conjugate gradient method, considering the following factors: inter-starting point distance, angles between tunnels, inter-tunnel distance, and the starting point's position relative to the base of the template (inside or outside). We established a semi-automatic design paradigm for fabricating three-dimensional printed template tailored for vaginal brachytherapy. While our initial findings are promising, further comprehensive investigations are imperative to validate the clinical efficacy of this innovative concept.

Introduction

Additive manufacturing, also known as three-dimensional (3D) printing technology, is a 3D modeling method that utilizes a series of techniques to fabricate objects by piling materials in successive layers. This technology is not limited to the manufacturing industry as it also used in the space and construction industries. In addition, it is becoming increasingly prevalent in the medical sector [1,2].

The combination of external beam radiotherapy and brachytherapy plays an important role in the treatment of primary vaginal tumors and vaginal recurrence of endometrial or cervical cancer after surgery [3–8]. Brachytherapy is a form of radiotherapy that involves the insertion of radioactive material such as seeds, wires, needles, catheters, or applicators into or near the tumor either temporarily or permanently. During brachytherapy for gynecological malignancies, templates, which can be either commercially obtained or fashioned in-house, are employed to assist in the placement of applicators, maintain a specific distance between the applicators, or secure the applicators during treatment. To

improve the fit of applicators, some researchers have proposed using customized templates for brachytherapy of vaginal tumors, created using 3D printing technology [9,10].

We were the first to publish a report on an inversely designed technique using 3D printing for creating templates for brachytherapy of gynecological malignancies [11]. Our method provided patient-specific templates, which lead to reduced insertion times during brachytherapy. However, a significant drawback was the manual and labor-intensive process of measuring and designing the templates.

To address this issue, we proposed a novel semi-automatic design concept for 3D-printed templates for brachytherapy for vaginal cuff tumors.

Technical note

Premise of tumor and template

This study specifically targeted tumors located at or near to the

* Corresponding author at: Department of Radiation Oncology, Osaka Police Hospital, 10-31, Kitayama-cho, Tennoji-ku Osaka, Osaka 543-0035, Japan.

E-mail address: ssekii@oph.gr.jp (S. Sekii).

<https://doi.org/10.1016/j.stlm.2024.100147>

Received 6 September 2023; Received in revised form 9 November 2023; Accepted 5 February 2024

Available online 5 February 2024

2666-9641/© 2024 The Authors. Published by Elsevier Masson SAS. This is an open access article under the CC BY license (<http://creativecommons.org/licenses/by/4.0/>).

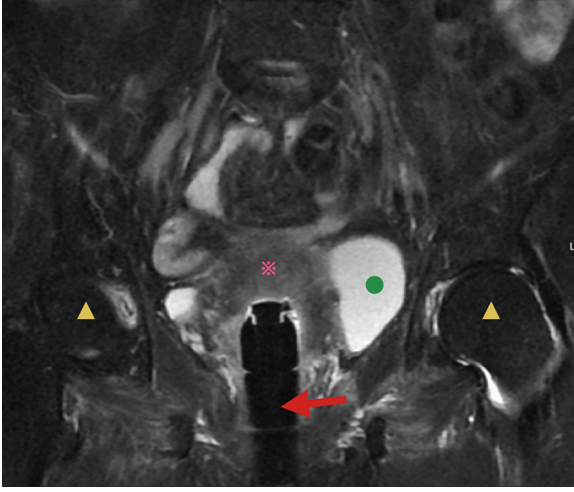


Fig. 1. Coronal T2-weighted magnetic resonance image of applicator used in vagina and surrounding organs and tumor. Red arrow, yellow triangles, and green circle designate a commercially available applicator, femoral heads, and bladder, respectively. Asterisk indicates a tumor.

vaginal cuff, while those located below this level were not considered. The template considered in the study was a composite of a right cylinder and a hemisphere, with a longitudinal length of 7 cm and a base diameter of 3 cm, and the circular parts of each shape were in contact with each other. The cylindrical component of the 3D shape was located caudally, whereas the hemispherical aspect was located cranially. To establish the spatial relationship between the tumor and the template, it was assumed that medical images were acquired prior to template design using a commercially available cylinder applicator (Elekta AB; Stockholm, Sweden) with the diameter of 3 cm that is inserted into the vagina. Fig. 1 was an example of magnetic resonance image of applicator used in vagina. The designed template was also intended to be used in a vaginally inserted position.

The design of the template was established by determining the tumor projection and the direction of applicator insertion based on specified the terminal and starting points at which the applicator initially traversed the template.

Projection of tumor

To confirm the orientation of the tumor relative to the template, a mask image extracted from the 3D tumor domain was projected onto the surface of a true sphere. The center of the sphere was aligned with the base of the cylindrical component of the template, and the radius was set between the center and the farthest point on the tumor (Figs. 2 and 3).

The function related to tumor projection was calculated as follows:

$$T_{\theta, \varphi} = \sum V_{\theta, \varphi}$$

Here, $V_{\theta, \varphi}$ is the voxel set of the medical image voxels on the line segment in the direction (θ, φ) from the center of the base of the cylindrical component of the template.

Terminal points

To determine the terminal points, candidate points were evenly distributed on the previously projected surface at fixed angle intervals. The projected points were then segmented into clusters using the k-means method, with the center of each cluster designated as the terminal point.

The projected points' group was calculated as:

$$P = \{T_{\theta, \varphi} | \theta \in \Theta, \varphi \in \Phi, T_{\theta, \varphi} > 0\}$$

Here, Θ and Φ are the values quantized every 1° from 0 to 2π (rad), respectively. The k-means method was employed to divide group P into k clusters, with the center of each cluster determined to be the terminal point.

Starting points

The centers of the sites where applicators first passed through the template were regarded as starting points. All starting points were located exclusively on the base of the cylinder and not on its lateral surface. The penetration of applicators from outside the template (e.g. transperineal approach) or through the lateral grooves of the cylindrical component, was not considered. Four factors were considered to determine the applicators' starting points. The first factor was the distance between the starting points.

The distance between the starting points was calculated as follows:

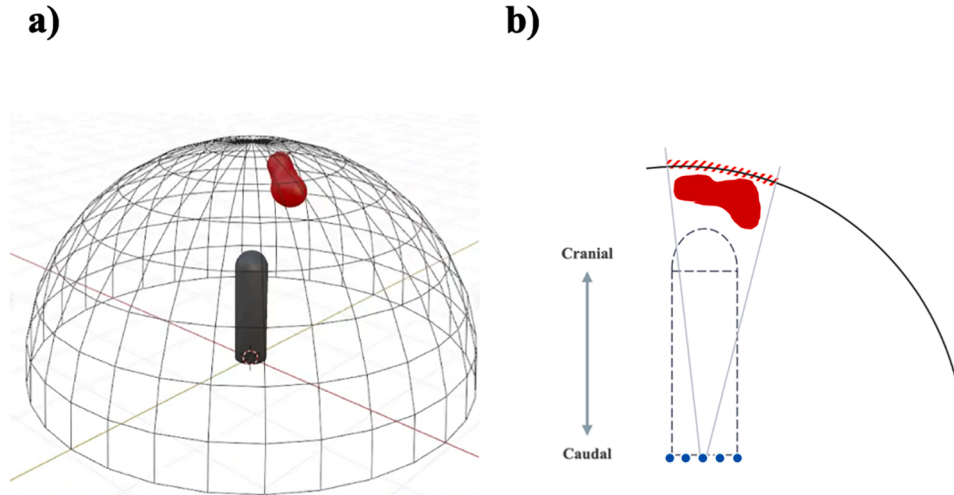


Fig. 2. Schematic diagram of tumor projection.

a) Tumor and template domains in the coordinate space. Red irregular shape indicates tumor domain. Black domain consisting of hemisphere and cylinder indicates template in vagina. b) Cross-sectional view in a plane parallel to the long axis direction of cylinder template. Figure marked by dotted line is a cylinder template, in the bottom of which, blue circles indicate starting points. Red shaded area indicates the projected tumor.

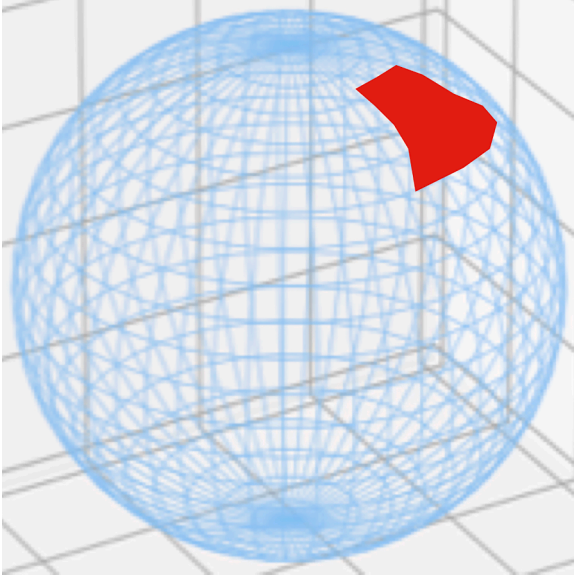


Fig. 3. Example of mask image.
Red area indicates mask image of tumor.

$$\hat{\delta}_p(\mathbf{S}) = \frac{1}{|\mathbf{S}|(|\mathbf{S}| - 1)} \sum_{s_1 \in \mathbf{S}} \sum_{s_2 \in \mathbf{S}} \delta(|s_1 - s_2|)$$

$$\delta(s) = \begin{cases} 0 & (s \geq d) \\ \frac{s-d}{d} & (s < d) \end{cases}$$

Here, s and d represent the distance between the two starting points and the diameter of the hole, respectively. Given that 6-French (2 mm) plastic needle applicators (ProGuide, Elekta, Sweden) were used, the size of each insertion tunnel through which these applicators passed within the template was set at 3 mm to allow for a margin, although 2.3 to 2.5 mm was sufficient based on past experience with acrylonitrile-butadiene-styrene (ABS) or polycarbonate / ABS (PC-ABS). The second and third factors were the angle and distance between the tunnels, respectively, to avoid tunnel crossing, because all the applicators were inserted one a time and were then simultaneously located *in situ* during brachytherapy.

Regarding the second factor, the angle between the tunnels, the group of vectors, \mathbf{V} , from starting point s to terminal point t is defined as:

$$\mathbf{V} = \{t - s \mid t \in \mathbf{T}, s \in \mathbf{S}\}$$

The angle between the tunnels was also taken into account to avoid an appearance of crossing when viewed from a certain direction, indirectly reducing the probability of crossing.

The angle of two vectors u and v for all combinations of the tunnels were calculated as:

$$\varphi(\mathbf{S}, \mathbf{T}) = \log \left\{ 1 + \frac{1}{|\mathbf{V}|(|\mathbf{V}| - 1)} \sum_{u \in \mathbf{V}} \sum_{v \in \mathbf{V}} \left\{ 1 - \frac{u \cdot v}{|u||v|} \right\} \right\}$$

The distance between the tunnel was calculated as:

$$\hat{\delta}_r(\mathbf{S}, \mathbf{T}) = \frac{1}{|\mathbf{S}|(|\mathbf{S}| - 1)} \sum_{s_1 \in \mathbf{S}} \sum_{s_2 \in \mathbf{S}} \delta\{\eta(s_1, t_1, s_2, t_2)\}$$

where η is the minimum distance between the two line segments from s_1 to t_1 and from s_2 to t_2 .

The fourth factor was to exclude cases where the starting point was outside the base of the cylinder.

The following function ξ assigns an infinite penalty to the starting

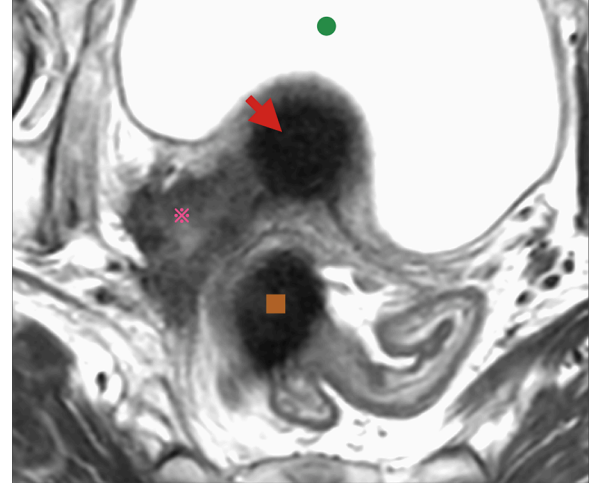


Fig. 4. Axial T2-weighted magnetic resonance image for simulation.
Red arrow, brown square, and green circle designate a commercially available applicator, rectum, and bladder, respectively. Asterisk indicates a tumor.



Fig. 5. Example of designed template.

point s when it satisfies the condition:

$$\xi(\mathbf{S}) = \sum_{s \in \mathbf{S}} \xi(s)$$

$$\xi(s) = \begin{cases} \infty & \left(R - |s - O| < \frac{d}{2} \right) \\ 0 & (\text{otherwise}) \end{cases}$$

where R is the radius of the cylinder, $|s - O|$ calculates the distance between the starting point s and cylinder center O .

The conjugate gradient method, implemented using Python SciPy module "scipy.optimize.minimize" was used to minimize an objective function containing these four factors. The functions of these four factors

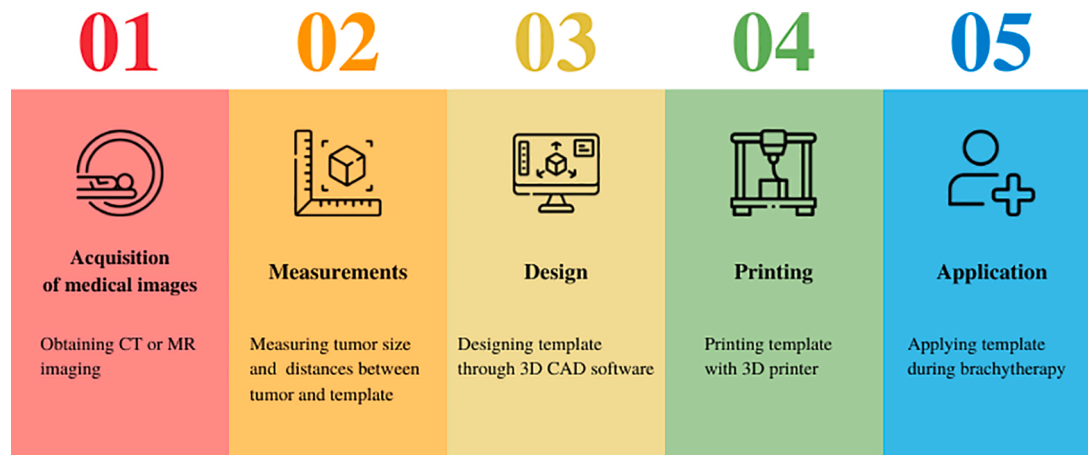


Fig. 6. Workflow of 3D printed template for brachytherapy.

were summed to create the following function:

$$f = \hat{\delta}_p(\mathbf{S}) + \varphi(\mathbf{S}, \mathbf{T}) + \hat{\delta}_r(\mathbf{S}, \mathbf{T}) + \xi(\mathbf{S})$$

Simulation

We conducted a simulation of the proposed method employing magnetic resonance images from a 67-year-old woman who had previously undergone hysterectomy for cervical cancer and was newly diagnosed with a vaginal tumor (Fig. 4).

The tumor was located in the right paracolpium, with a maximum size of 2.8 cm.

Fig. 5 illustrates a template that was designed in accordance with instructions to generated 9 tunnels.

Ethical statement

All researchers involved in this study acted and performed the study according to the Declaration of Helsinki and Ethical guidelines for medical and health research involving human subjects. The study was granted approval by the institutional ethical committee, and informed consent was obtained from a participant.

Discussion

To the best of our knowledge, this study represents the first report on the semi-automatic designing of 3D-printed templates for brachytherapy of gynecological carcinomas. Currently, commercially available templates for brachytherapy of vaginal tumors are limited. Cylindrical templates/applicators such as a Vaginal CT/MR applicator (Elekta AB, Stockholm, Sweden) are frequently used to treat superficial vaginal tumors localized to 5 mm deep within the vaginal wall. However, for large tumors with paravaginal tissue invasion, needle applicators inserted through transperineal or transvaginal approaches are often selected to treat the entire tumor, and perineal templates, such as the Syed/Neblett GYN template (Best Medical International, Inc., Springfield, VA, USA) and Martinez Universal Perineal Interstitial Template (Elekta AB, Stockholm, Sweden) are commonly used. However, these templates offer limited flexibility in terms of insertion position, which can make insertion of applicators from the appropriate position and placement within the correct region time consuming. In contrast, the freehand insertion technique, without templates, also depends on the experience of the individual brachytherapists. Our method could facilitate inexperienced brachytherapists to surpass the threshold of interstitial brachytherapy for vaginal tumors.

With the growing trend of 3D printing technology in medicine, the convergence of this technology with brachytherapy may seem less

revolutionary, but emerging research suggests potential benefits. A systematic review of 3D printing in radiation oncology revealed that the most common applications in clinical settings pertain to brachytherapy applicators [12]. 3D printing technology can improve workflow and enhance the versatility of catheter tunnels in brachytherapy. The phases involved in fabricating a template with a 3D printer before its application in brachytherapy were as follows: (1) acquisition of medical images, (2) measurements, (3) design, and (4) printing (Fig. 6).

While the problem in the printing phase can be resolved by using a 3D printer instead of outsourcing the print, challenges in the measurement and design phases still remain. Although our method still requires delineation of the tumor and visual inspection to ensure the proper placement of the tunnels, we anticipate that automating other aspects of the measurement and design phases will not only substantially reduce the time required for these phases, but also decrease the likelihood of tumor size changes and unsuitable template fabrication for optimal brachytherapy planning. In the future, the convergence of our concept with automatic contouring from medical images is anticipated to further optimize the first four phases.

The four factors utilized in our method fulfill the necessary conditions for semi-automatic template design. In a report by Zhang et al. on preplan-based 3D personalized template-guided brachytherapy for cervical cancer, the authors considered manually designed the insertion tunnels based on five principles: (1) minimum inter-tunnel distance on the transverse section, (2) the minimum inter-starting point distance, (3) the interference between oblique and parallel tunnels, (4) the minimal number of oblique tunnels, and (5) the distance between the terminal points and clinical target volume or organ at risk [13]. Our first three factors, which include the inter-starting point distance, angles between each tunnel, and inter-tunnel distance, align with their first three principles. Therefore, we consider these factors to be reasonable conditions. Our fourth factor, which excludes starting point located outside the base of the cylinder, represents a distinctive condition. Although it is possible to insert through the template side by avoiding the mucosa or labia minora near the introitus or via the vulva, we chose to impose this condition to demonstrate the feasibility of fabricating a cylindrical template under such stringent conditions. Considering the variations in tumor topography or geometry, it is possible that simply creating multiple tunnels within the limited volume of the cylindrical shape may not provide adequate applicator positions. Hence, further studies are needed to investigate automated template designs that conform to the curvature of the vulva to address such scenarios.

Our study had some limitations. First, the design was limited to the materials we previously used, limiting its applicability to other materials. Additionally, the calibration process requires the adjustment of the values within each factor. Second, the template has a fixed size. As the

size of the template varies among patients, the numerical values in the formulas must be adjusted accordingly every time. Third, our study did not consider the existence of organs at risk, such as the bladder and rectum. We plan to incorporate this information into the formula in future studies. Fourth, the appropriate number of tunnels for each patient was not established. Although a single combination of tunnels would be ideal, the determination of the number of tunnels currently relies on assessments by skilled brachytherapists. Fifth, differences in vaginal distortion between the design and the application phases were not considered. Although our study attempted to minimize this issue by employing a commercially available cylinder with a diameter similar to designed template, it is crucial to acknowledge that differences may occur.

Further validation is needed to establish the reliability of the utility of this concept in real-world clinical practice.

Conclusions

Our study conceptualized a semi-automatic design of a 3D-printed, individualized template for interstitial brachytherapy of vaginal tumors. Further validation of this concept is necessary in clinical practice. We anticipate that converging this concept with automatic contouring from medical imaging will enhance efficiency in the future.

Declaration of competing interest

The authors declare no conflicts of interest associated with this manuscript.

Acknowledgment

S.S. and K.M. contributed equally to this work. Icon images from Flaticon.com was used for part of the figures. We thank the staffs involved in this study for their support.

References

- [1] Diment LE, Thompson MS, Bergmann JHM. Clinical efficacy and effectiveness of 3D printing: a systematic review. *BMJ Open* 2017;7:e016891.
- [2] Hong D, Lee S, Kim T, Baek JH, Lee YM, Chung KW, Sung TY, Kim N. Development of a personalized and realistic educational thyroid cancer phantom based on CT images: an evaluation of accuracy between three different 3D printers. *Comput Biol Med* 2019;113:103393.
- [3] Jhingran A, Burke TW, Eifel PJ. Definitive radiotherapy for patients with isolated vaginal recurrence of endometrial carcinoma after hysterectomy. *Int J Radiat Oncol Biol Phys* 2003;56:1366–72.
- [4] Sekii S, Murakami N, Kato T, Harada K, Kitaguchi M, Takahashi K, Inaba K, Igaki H, Ito Y, Sasaki R, Itami J. Outcomes of salvage high-dose-rate brachytherapy with or without external beam radiotherapy for isolated vaginal recurrence of endometrial cancer. *J Contemp Brachytherapy* 2017;9:209–15.
- [5] Concin N, Matias-Guiu X, Vergote I, Cibula D, Mirza MR, Marnitz S, Ledermann J, Bosse T, Chagari C, Fagotti A, Fotopoulou C, Gonzalez Martin A, Lax S, Lorusso D, Marth C, Morice P, Nout RA, O'Donnell D, Querleu D, Raspollini MR, Sehouli J, Sturdza A, Taylor A, Westermann A, Wimberger P, Colombo N, Planchamp F, Creutzberg CL. ESGO/ESTRO/ESP guidelines for the management of patients with endometrial carcinoma. *Int J Gynecol Cancer* 2021;31:12–39.
- [6] Murakami N, Kato T, Miyamoto Y, Nakamura S, Wakita A, Okamoto H, Tsuchida K, Kashiwara T, Kobayashi K, Harada K, Kitaguchi M, Sekii S, Takahashi K, Umezawa R, Inaba K, Ito Y, Igaki H, Itami J. Salvage high-dose-rate interstitial brachytherapy for pelvic recurrent cervical carcinoma after hysterectomy. *Anticancer Res* 2016;36:2413–21.
- [7] Amsbaugh MJ, Bhatt N, Hunter T, Gaskins J, Parker L, Metzinger D, Amsbaugh A, Sowards K, El-Ghamry M. Computed tomography planned interstitial brachytherapy for recurrent gynecologic cancer. *Brachytherapy* 2015;14:600–5.
- [8] Murakami N, Kasamatsu T, Sumi M, Yoshimura R, Takahashi K, Inaba K, Morota M, Mayahara H, Ito Y, Itami J. Radiation therapy for primary vaginal carcinoma. *J Radiat Res* 2013;54:931–7.
- [9] Wiebe E, Easton H, Thomas G, Barbera L, D'Alimonte L, Ravi A. Customized vaginal vault brachytherapy with computed tomography imaging-derived applicator prototyping. *Brachytherapy* 2015;14:380–4.
- [10] Sethi R, Cunha A, Mellis K, Siau T, Diederich C, Pouliot J, Hsu IC. Clinical applications of custom-made vaginal cylinders constructed using three-dimensional printing technology. *J Contemp Brachytherapy* 2016;8:208–14.
- [11] Sekii S, Tsujino K, Kosaka K, Yamaguchi S, Kubota H, Matsumoto Y, et al. Inversely designed, 3D-printed personalized template-guided interstitial brachytherapy for vaginal tumors. *J Contemp Brachytherapy* 2018;10:470–7.
- [12] Rooney MK, Rosenberg DM, Braunstein S, Cunha A, Damato AL, Ehler E, Pawlicki T, Robar J, Tatebe K, Golden DW. Three-dimensional printing in radiation oncology: a systematic review of the literature. *J Appl Clin Med Phys* 2020;21:15–26.
- [13] Zhang B, Zhang S, Sun L, Wu Y, Yang Y. Characteristics of preplan-based three-dimensional individual template-guided brachytherapy compared to freehand implantation. *J Appl Clin Med Phys* 2022:e13840.